The influence of OH groups on the growth of rhodium on alumina: a model study

M. Heemeier, M. Frank, J. Libuda, K. Wolter, H. Kuhlenbeck, M. Bäumer * and H.-J. Freund

Fritz-Haber-Institut der Max-Planck-Gesellschaft, Faradayweg 4-6, 14195 Berlin, Germany
E-mail: baeumer@fhi-berlin.mpg.de

Received 8 February 2000; accepted 25 May 2000

In order to investigate how the presence of surface hydroxyl groups on oxide surfaces affects the interaction with the supported metal, we have modified a well-ordered alumina film on NiAl(110) by Al deposition and subsequent exposure to water. This procedure yields a hydroxylated alumina surface as revealed by infrared and high-resolution electron energy loss spectroscopy. By means of scanning tunneling microscopy, we have studied the growth of rhodium on the modified film at 300 K. Clear differences in the particle distribution and density are observed in comparison to the clean substrate. While, in the latter case, decoration of domain boundaries as typical defects of the oxide film governs the growth mode, a more isotropic island distribution and a drastically increased particle density is found on the hydroxylated surface. From infrared data, it can be deduced that the growth is connected with the consumption of the hydroxyl groups due to the interaction between the metal deposit and the hydroxylated areas. This finding is in line with photoemission results published earlier.

Keywords: aluminum oxide, hydroxyl groups, rhodium, growth, scanning tunneling microscopy, infrared spectroscopy

1. Introduction

Alumina substrates, which are used, for example, as support materials in heterogeneous catalysis, exhibit a rather complex surface chemistry [1]. Depending on the preparation procedure, the surface properties can be governed by co-ordinatively unsaturated O^{2-} ions (Lewis basic sites) and Al^{3+} ions (Lewis acidic sites). Of particular interest, however, is the role of surface hydroxyl groups, which are usually present in varying concentration. Apart from their influence on the surface structure [2,3] and adsorption properties of the support, OH groups may act as mediators for strong metal–oxide interactions. Here, one of the best known examples is the CO-induced Rh redispersion [4–7], which, on alumina substrates, has been shown to involve hydroxyl species [6].

In contrast to technical alumina supports, model systems based on ordered oxide films have the advantage of being easily accessible to most surface science probes and providing well-defined surface properties [8–11]. In order to elucidate the possible role of OH groups for the growth and the interaction of rhodium with alumina supports, we have used a well-ordered thin Al_2O_3 film grown on NiAl(110) [12]. In its pristine form, the film is OH-free and probably oxygen-terminated (quasi-hexagonal arrangement of oxygen ions at the surface) [10]. As described in the following, it can be hydroxylated in a controllable way by a modification procedure based on aluminum deposition and subsequent exposure to water.

In a preceding paper, we have already presented first high-resolution LEED (low-energy electron diffraction) and XPS (X-ray photoelectron spectroscopy) results concerning the growth of Rh on this modified surface [13]. Here, we will discuss complementary new STM (scanning tunneling microscopy) data showing in detail the changes in nucleation behaviour on the microscopic level. Since the growth of Rh on the unmodified film has already been studied before [10,14], we are in the position to make a direct comparison between the behaviour on the OH-free and the OH-terminated surface. Strong differences with respect to nucleation are found, as discussed in section 3. As revealed by infrared and high-resolution XP spectra for both the alumina and Rh core levels, this is connected with a consumption of the OH groups.

2. Experimental

Except for the HREELS (high-resolution electron energy loss spectroscopy) experiments, the results presented here have been obtained in a multi-chamber UHV (ultrahigh vacuum) system equipped with an Omicron variable temperature STM (operated at room temperature) and a Bruker IFS 66v infrared spectrometer. The latter instrument is operated in reflection geometry (angle of incidence: 84°) and was set to a spectral resolution of about 2 cm^{-1}. The system furthermore contains an X-ray gun and a hemispherical analyser (Scienta) for photoelectron spectroscopy as well as all instruments for the sample preparation including gas dosers and metal evaporators (see below). The sample was mounted on a sample carrier allowing the transfer between

* To whom correspondence should be addressed.

the different experimental stages. In order to control the crystal temperature, a NiCr/Ni thermocouple spot-welded to the sample was used.

The HREELS data have been taken in a UHV system with a VSI Delta 0.5 instrument (resolution limit: 0.5 meV = 4 cm^{-1}). All spectra have been recorded in specular geometry with an energy resolution of 1.4–2.5 meV and count rates of 200 kHz at a primary energy of 5–7 eV. In this chamber, the sample was spot-welded to two Ta wires which, in turn, were spot-welded to two W rods. Again, a NiCr/Ni thermocouple was used to monitor the crystal temperature.

The clean NiAl(110) surface was prepared by several cycles of sputtering (Ar^+ ions, 1.5 keV) and annealing to 1300 K. The ordered Al_2O_3 film was obtained as previously reported in the literature [12]. After dosing about 5000 L O_2 (1 L = 10^{-6} Torr s^{-1}) at a sample temperature of 550 K, the crystal was briefly annealed to 1250 K. The quality of the oxide was checked by STM as well as via its phonon bands in the infrared and HREEL spectra.

Aluminum was deposited by a home-built evaporator source with a small resistively heated alumina crucible. The evaporator was calibrated using a quartz microbalance. Typical evaporation rates amounted to 0.8 Å Al min^{-1} (1 Å Al corresponds to 6.1×10^{14} atoms cm^{-2}). Rh was evaporated from a rod (Heraeus, >99.9%) using a commercial electron bombardment evaporator (EMF 3, Omicron). During deposition, the crystal was biased with a retarding voltage in order to avoid ion acceleration towards the sample (point defect creation). The flux was calibrated by a quartz microbalance prior to use and checked by STM (deposition of submonolayer amounts of the metal on the clean NiAl crystal where a layer-by-layer growth is observed). The evaporation rate was chosen to be 0.8 Å Rh min^{-1} (1 Å Rh corresponds to 7.3×10^{14} atoms cm^{-2}). In the following, the *nominal film thickness* as obtained by the microbalance is used to quantify the amounts of metal deposited.

3. Results and discussion

The most straightforward way to prepare hydroxylated alumina surfaces certainly is direct exposure to water vapour. Although this procedure is successful in some cases [15–20], in the case of the ordered Al_2O_3 film on NiAl(110) very large exposures are required to induce detectable changes, e.g., in the LEED pattern. Therefore, we have chosen a different pathway by (***A***) preparing the clean oxide film, (***B***) evaporation of metallic Al at 300 K and (***C***) exposure to water at 90 K and subsequent annealing to 300 K in order to desorb the molecularly adsorbed water. Water is known to dissociate and oxidise Al under these conditions [21]. This modified surface is finally used as a substrate for Rh deposition.

Previously, we have characterised the different stages of preparation with respect to their geometric and electronic structure employing SPA-LEED (spot-profile analysis of electron diffraction spots) in conjunction with PES (photoelectron spectroscopy) [13]. Here, we report the results of additional STM and IRAS (infrared reflection absorption spectroscopy) studies and reconsider the PE results with regard to the Rh growth on this support.

3.1. Characterisation of the modified Al_2O_3 film

In figure 1(A), an STM picture (0.5 μm × 0.5 μm) of the non-modified Al_2O_3/NiAl(110) surface is presented (situation ***A***). The oxide film is atomically flat and well-ordered even on a large scale. Although a few monoatomic substrate steps can be identified, the dominating defect structure is a network of domain boundaries visible as protruding lines in the STM image. In fact, the network consists of two types of domain boundaries, as revealed by the close up in figure 1(B): reflection domain boundaries (A–B), separating areas of different azimuthal orientation, and antiphase domain boundaries denoted (A–A) and (B–B), which ap-

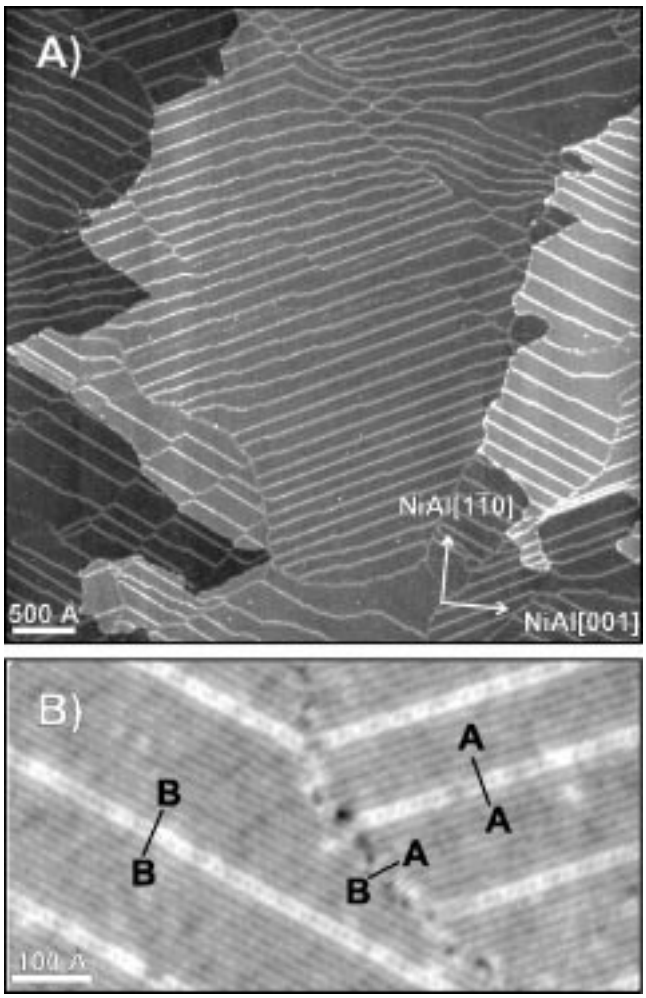

Figure 1. (A) STM image of the non-modified alumina film grown on NiAl(110) (CCT (constant current topography), 5000 Å × 5000 Å, U_{tip} = −3.05 V, I = 0.057 nA); (B) Close-up showing the various domain boundaries in more detail (CCT, 775 Å × 400 Å, U_{tip} = −4.0 V, I = 0.5 nA): A–A, B–B – antiphase domain boundaries, A–B – reflection domain boundary.

pear as bright double lines in the image. While the growth of two reflection domains is due to the twofold symmetry of the NiAl(110) support, the antiphase domain boundaries are the result of a lateral displacement (lattice mismatch) between two adjacent oxide areas. As seen in figure 1 and discussed in detail elsewhere, they usually grow in a parallel fashion with an average distance of the order of 100–200 Å [10,22].

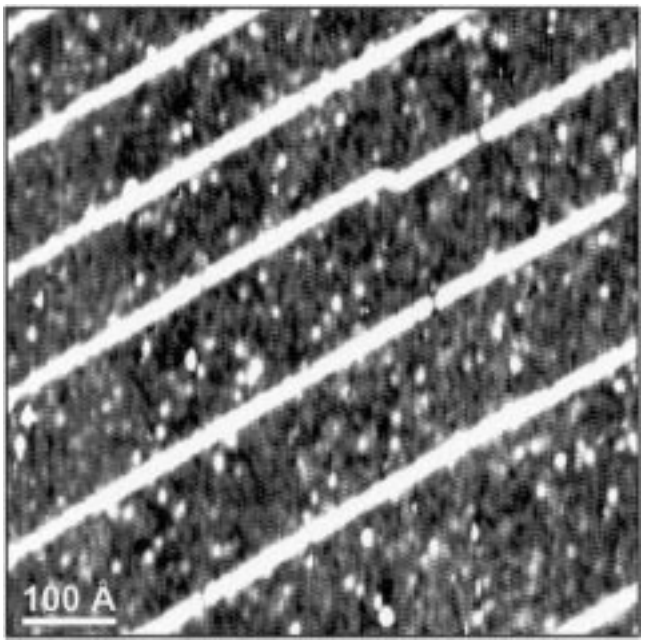

Figure 2. STM image taken after deposition of 0.02 Å Al onto Al_2O_3/NiAl(110) at 300 K (CCT, 670 Å × 670 Å, $U_{tip} = -2.9$ V, $I = 0.05$ nA).

For the situation ***B***, i.e., after Al deposition at 300 K, previous SPA-LEED studies have provided evidence of a high density and an isotropic distribution of Al aggregates on the film. In particular, no apparent decoration of the oxide defect structure was observed [13]. Although it turned out to be very difficult to obtain stable tunneling conditions for this situation, STM corroborates this interpretation. A corresponding image is depicted in figure 2, showing that the Al deposits are highly dispersed and evenly distributed on the surface. From STM images taken *after* water exposure, we conclude that no drastic morphological changes occur upon this treatment. This is also consistent with SPA-LEED results that likewise suggest a negligible effect of the oxidation/hydroxylation procedure on the surface morphology.

In order to check the successful generation of OH groups on the film, infrared and electron energy loss spectroscopic measurements have been carried out which are presented in figure 3. After deposition of 1 Å Al and exposure to water at 90 K, a spectrum typical of a thick ice layer is observed

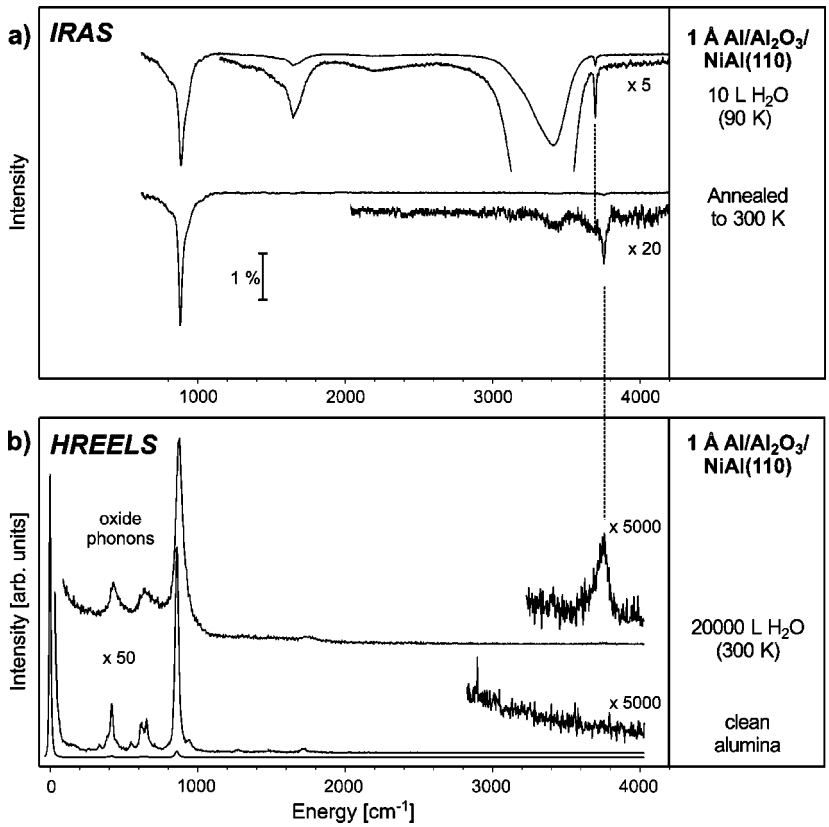

Figure 3. (a) IR spectrum recorded after deposition of 1 Å Al onto the alumina film at 300 K and subsequent exposure to water at 90 K (top) as well as a spectrum recorded after further heating to 300 K and cooling to 90 K again (bottom). (A small contribution due to water condensation in the IR detector has been subtracted from the latter spectrum.) (b) HREEL spectrum recorded after deposition of 1 Å Al onto the alumina film and subsequent treatment with water at 300 K. The spectrum of the non-modified film is shown for comparison.

with IRAS (figure 3(a)) [23] in addition to a phonon band of the alumina film (see [12] and HREEL spectrum below). While most of the absorption bands are rather broad, a sharp peak is discernible at 3698 cm^{-1} which is due to the OH streching mode of free, non-hydrogen-bonded OH groups on the surface of the ice layer [24,25]. When this system is heated to 300 K and cooled down to 90 K again (***C***), a new sharp feature appears at 3756 cm^{-1} in good agreement with OH streching signals on hydroxylated alumina bulk substrates and films [17–19]. According to Knözinger et al. [26], the position of the band points to OH groups terminally or bridge-bonded to Al ions residing in three-fold hollow sites on the surface. Apart from the new peak, weak bands of water are still observable in the spectrum as a result of unavoidable water re-adsorption.

The HREELS data displayed in figure 3(b) fully confirm the IRAS results. In this case, the hydroxylation of the Al deposits with water has been carried out directly at room temperature. The treatment results in a feature at virtually the same position as in the infrared spectrum, i.e., at 465 meV = 3748 cm^{-1}.

The comparatively low intensity of this peak as well as of the IR band might lead to the suspicion that the amount of OH groups formed by our procedure is rather small. This, however, is not the case. On the one hand, similarly low intensities have been observed in other studies on hydroxylated alumina surfaces as well [17,18]. On the other hand, XPS data discussed previously are incompatible with such a conclusion. Here, the three-step preparation gives rise to a new feature at higher binding energy in the O 1s spectrum (see figure 5) the intensity of which points to an appreciable amount of OH species on the surface.

3.2. Rh growth on the modified Al_2O_3 film

Before we discuss the nucleation and growth of Rh on the modified film ***C***, we will give a brief review of the behaviour on the clean Al_2O_3/NiAl(110) surface ***A*** (for a more detailed description of this system see [10,14]). Figure 4 (top) contains an STM image taken after deposition of 0.2 Å Rh at 300 K. At this surface temperature, an efficient decoration of the oxide domain boundaries and steps is found, as indicated by the formation of characteristic chains of particles along the line defects. Only on larger domains do a few aggregates grow on the domains themselves [10]. The average island density for the situation displayed in figure 4, top, is about 2.5×10^{12} cm^{-2}, corresponding to an average island size of approximately 100 atoms/island.

If we now turn to the remaining STM images in figure 4, elucidating the Rh growth on the modified film (***C***), clear differences are detectable with respect to the nucleation behaviour. The data presented there have been obtained with *a constant amount of Rh (0.2 Å)*, but an increasing amount of Al deposited during step ***B***. On the basis of these results, the following conclusions can be drawn:

- The domain boundaries lose their significance as preferred nucleation sites upon raising the Al (pre)coverage. An increasing number of particles can be found within the domains now.

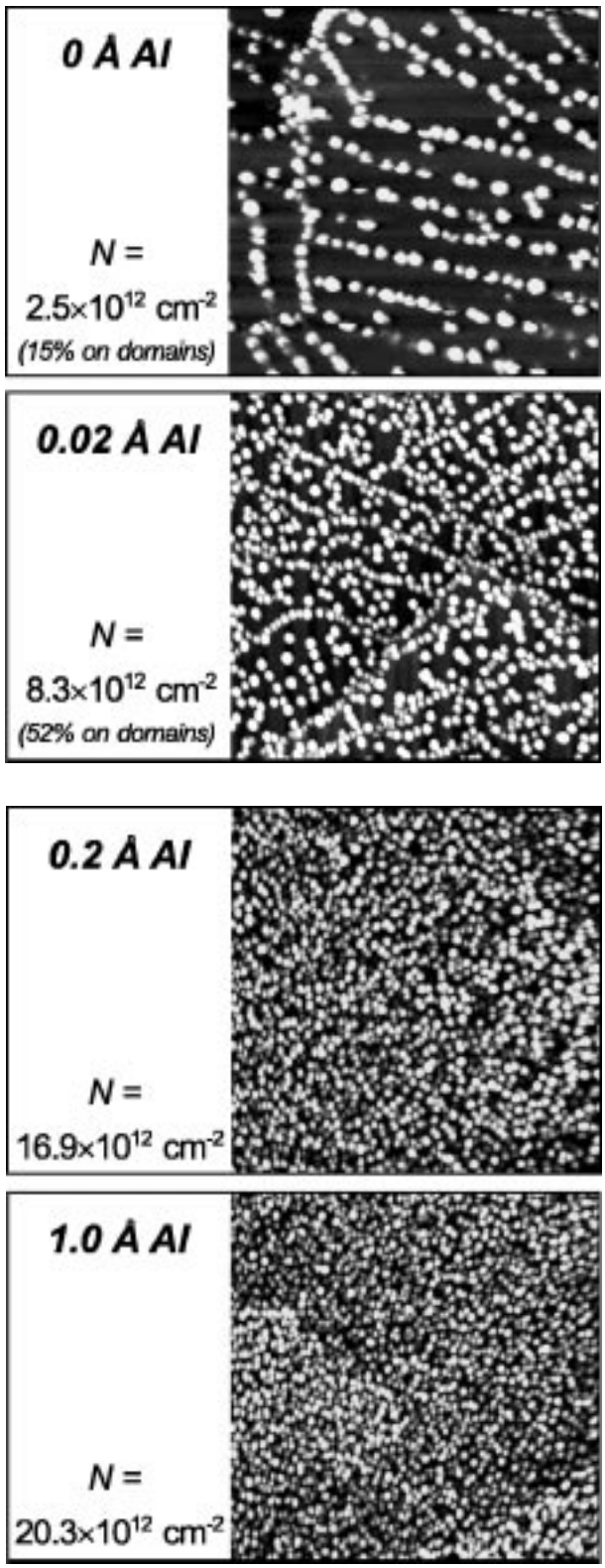

Figure 4. Series of STM images (CCT, 1000 Å × 1000 Å) taken after deposition of 0.2 Å Rh onto the original (topmost image) and modified alumina film at 300 K (N = density of Rh particles). The amount of Al used for the modification procedure varied between 0.02 and 1.0 Å Al.

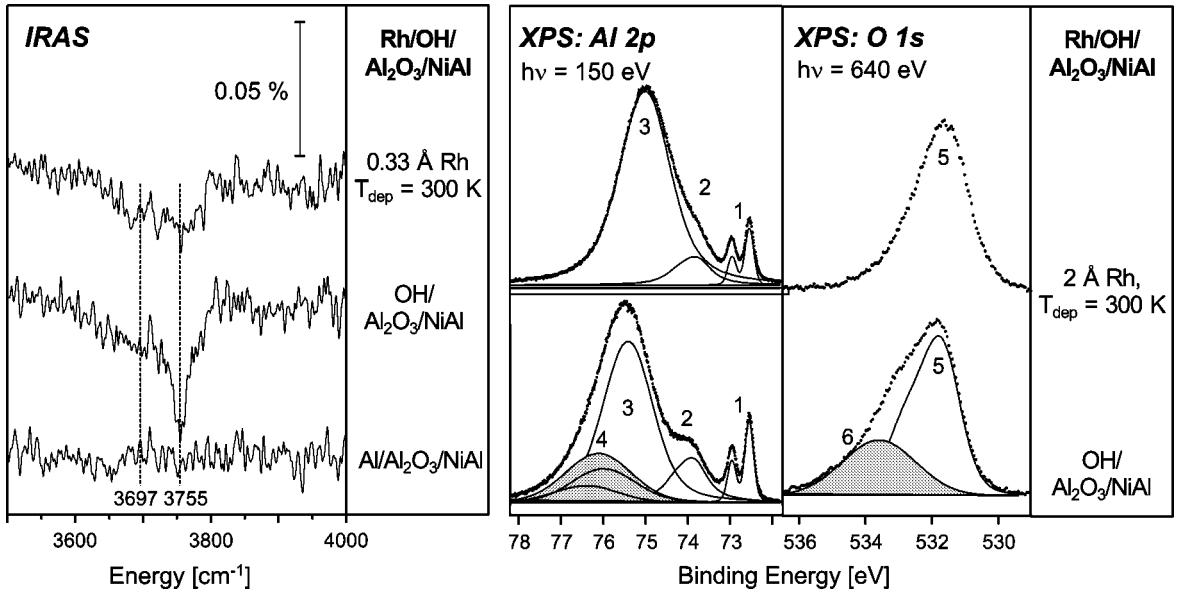

Figure 5. IR spectra of the OH streching region (left) as well as Al 2p and O 1s photoelectron spectra in normal emission geometry (right, from [13]) taken before and after deposition of Rh onto the modified alumina film at 300 K (deposition of 1 Å Al and exposure to 10 L H_2O). The IR spectrum recorded before water exposure is shown for comparison. Assignments for the Al 2p and O 1s components 1–6 are given in the text.

- Due to this fact, the island density increases to $\sim 2 \times 10^{13}$ cm^{-2} for 1 Å Al resulting in particles of about 10 atoms/island.

These observations are consistent with our previous SPA-LEED results, which suggested a comparable island density and a homogeneous particle distribution on the surface [13].

Although STM obviously reveals a modified nucleation behaviour, it cannot shed light on the nature of the chemical interaction between the metal and the hydroxylated areas. Infrared spectra and PES measurements that are compiled in figure 5 have answered this question. Both experiments clearly show that the metal deposit in fact consumes the OH groups. In the IR spectra, the intensity of the OH streching signal due to the surface hydroxyl groups is considerably reduced even for small amounts of Rh deposited at 300 K.

In the case of the PES data, a comparison of the Al 2p and O 1s spectra for the hydroxylated film ***C*** before and after Rh deposition provides information about this aspect. At first, the Al 2p spectrum of hydroxylated Al_2O_3/NiAl(110) consists of four spin–orbit split components (see figure 5). The first three, which are also present for the non-modified film, can be assigned to the NiAl substrate (component 1), the substrate–oxide interface (component 2) and the oxide film (component 3). The fourth component at a binding energy (BE) of 76.0 eV as well as an additional high BE component in the O 1s region due to OH (component 6) are characteristic features of the hydroxylated surface. Similar high BE components have also been detected for other hydroxylated oxide surfaces [27–29].

Upon Rh exposure, two effects can be observed. In the first place, there is a shift of the oxide-related features to lower binding energy (Al 2p, component 3, and O 1s, component 5) due to a combination of electrostatic effects and increased final state screening [13]. More important for the following discussion, however, is the second effect, i.e., the changes in the characteristic high BE components of the modified film. Both the Al 2p and the O 1s features (components 4 and 6) completely disappear after metal deposition. A closer inspection of the substrate and oxide Al 2p intensity reveals that this effect cannot simply be caused by attenuation due to the Rh film. Instead, it must originate from a drastic shift to lower BE resulting in a coincidence with the original oxide emissions. Thus, the XPS results also prove a strong interaction of Rh with the OH-covered areas, a conclusion which is also confirmed by positive BE shifts in the Rh 3d region (not shown here) [13].

We, therefore, suggest that – in contrast to the oxygen-terminated surface, where no comparable effects are observed – the surface hydroxyl groups mediate a strong chemical interaction with the Rh metal. Schematically, we could describe the process as $\{Al^{3+}OH^{-}\} + Rh^0 \rightarrow \{Al^{3+}O^{2-}\} + Rh^{+} + H_{(ads)}$ resulting in the formation of a fraction of positively charged Rh species and in the consumption of OH during the deposition process.

4. Conclusions

We have studied nucleation and growth of Rh on a thin alumina film which was modified by deposition of metallic Al at 300 K followed by adsorption of water. According to our IRAS and HREELS data, this treatment results an a hydroxylated alumina surface. STM measurements demonstrate that the growth of Rh on this support strongly differs from the behaviour on the non-modified substrate. A drastically increased island density is observed which is dependent on the amount of Al deposited before. IRAS and PES data suggest that in contrast to the oxygen-terminated

alumina film, growth on the hydroxylated surfaces is connected with a strong chemical interaction in the course of which the surface hydroxyl groups are consumed.

Acknowledgement

Financial support of the following agencies is gratefully acknowledged: Deutsche Forschungsgemeinschaft, Bundesministerium für Bildung und Wissenschaft and Fonds der chemischen Industrie. Synetix, a member of the ICI group, through their Strategic Research Fund, has also supported this work. MF thanks the Studienstiftung des deutschen Volkes for a fellowship.

References

[1] A.B. Stiles, ed., *Catalyst Supports and Supported Catalysts* (Butterworth, Boston, 1987).
[2] D. Cappus, M. Haßel, E. Neuhaus, M. Heber, F. Rohr and H.-J. Freund, Surf. Sci. 337 (1995) 268.
[3] F. Rohr, K. Wirth, J. Libuda, D. Cappus, M. Bäumer and H.-J. Freund, Surf. Sci. 315 (1994) L977.
[4] H.F.J. van't Blik, J.B.A.D. van Zon, T. Huizinga, J.C. Vis and D.C. Koningsberger, J. Phys. Chem. 87 (1983) 2264; J. Am. Chem. Soc. 107 (1985) 3139.
[5] F. Solymosi and M. Pásztor, J. Phys. Chem. 89 (1985) 4789.
[6] P. Basu, D. Panayotov and J.T. Yates, Jr., J. Phys. Chem. 91 (1987) 3133; J. Am. Chem. Soc. 110 (1988) 2074.
[7] F. Solymosi and H. Knözinger, J. Chem. Soc. Faraday Trans. 86 (1990) 389.
[8] C.R. Henry, Surf. Sci. Rep. 31 (1998) 231.
[9] H.-J. Freund, Angew. Chem. Int. Ed. Engl. 36 (1997) 452.
[10] M. Bäumer and H.-J. Freund, Prog. Surf. Sci. 61 (1999) 127.
[11] D.W. Goodman, Surf. Rev. Lett. 2 (1995) 9; Surf. Sci. 299/300 (1994) 837.
[12] R.M. Jaeger, H. Kuhlenbeck, H.-J. Freund, M. Wuttig, W. Hoffmann, R. Franchy and H. Ibach, Surf. Sci. 259 (1991) 235.
[13] J. Libuda, M. Frank, A. Sandell, S. Andersson, P.A. Brühwiler, M. Bäumer, N. Mårtensson and H.-J. Freund, Surf. Sci. 384 (1997) 106.
[14] M. Bäumer, M. Frank, J. Libuda, S. Stempel and H.-J. Freund, Surf. Sci. 391 (1997) 204.
[15] D.B. Almy, D.C. Foyt and J.M. White, J. Electron Spectrosc. Relat. Phenom. 11 (1977) 129.
[16] J. Paul and F.M. Hoffmann, J. Phys. Chem. 90 (1986) 5321.
[17] J.G. Chen, J.E. Crowell and J.T. Yates, Jr., J. Phys. Chem. 84 (1986) 5906.
[18] V. Coustet and J. Jupille, Surf. Sci. 307–309 (1994) 1161.
[19] B.G. Frederick, G. Apai and T.N. Rhodin, Surf. Sci. 244 (1991) 67.
[20] M.A. Schildbach and A.V. Hamza, Surf. Sci. 282 (1993) 306.
[21] J.G. Chen, P. Basu, L. Ng and J.T. Yates, Jr., Surf. Sci. 194 (1988) 397.
[22] J. Libuda, F. Winkelmann, M. Bäumer, H.-J. Freund, Th. Bertrams, H. Neddermeyer and K. Müller, Surf. Sci. 318 (1994) 61.
[23] F. Franks, in: *Water. A Comprehensive Treatise, The Physics and Physical Chemistry of Water*, Vol. 1, ed. F. Franks (Plenum, New York, 1972) p. 115.
[24] B.W. Callen, K. Griffiths and P.R. Norton, Surf. Sci. Lett. 261 (1992) L44.
[25] B. Rowland and J.P. Devlin, J. Chem. Phys. 94 (1991) 812.
[26] H. Knözinger and P. Ratnasamy, Catal. Rev. Sci. Eng. 17 (1978) 31.
[27] V. Coustet and J. Jupille, Surf. Interface Anal. 22 (1994) 280.
[28] D. Cappus, C. Xu, D. Ehrlich, B. Dillmann, C.A. Ventrice, Jr., K. Al-Shamery, H. Kuhlenbeck and H.-J. Freund, Chem. Phys. 177 (1993) 533.
[29] L.-Q. Wang, D.R. Baer, M.H. Engelhard and A.N. Shultz, Surf. Sci. 344 (1995) 237.